JOURNAL OF MODERN OPTICS, 2001, VOL. 48, NO. 10, 1597-1615

Dispersion relation of surface plasmons near photonic band gaps: influence of the interaction with light

V. N. KONOPSKY and E. V. ALIEVA

Institute of Spectroscopy, Russian Academy of Sciences, Troitsk, Moscow region, 142190, Russia

(*Received 4 December 2000; revision received 5 March 2001*)

Abstract. We present an experimental and theoretical study of the photonic band gap in the propagation of surface plasmons (SPs) on periodically corrugated surfaces. Our main purpose is to investigate the case where the band gap width is larger than the energy distance between the SP dispersion curve for a flat surface and the light line. We introduce a physical model of the interaction of light waves with SPs and derive an analytical expression for the SP wave vector near band gaps based on the coupled-mode approach involving three interacting modes (two of them are SP modes and one is a light mode). By using the interferometric measurement we have studied, for the first time, the SP propagation parameters in the vicinity of the photonic band gap (10 μm wavelength region). The predictions of our theory are in good agreement with the experimental data.

1. Introduction

In recent years the optical properties of materials that possess a periodic modulation of their refraction index on the scale of the wavelength of light have received much attention [1]. Such materials can exhibit photonic band gaps that are very much like the electronic band gaps for electron waves travelling in the periodic potential of a crystal. In both cases frequency intervals exist where wave propagation is forbidden. Materials with band gaps for propagation of bulk light waves are called 'photonic crystals'. Surfaces that produce such a band gap for propagation of surface modes are called 'photonic surfaces' [2]. We will concentrate our discussion on the type of surface wave known as the surface plasmon (SP). The SP is a non-radiative transverse magnetic mode at a metal-dielectric interface [3]. The dispersion relation (the wave vector of the SP as a function of its frequency) at the metal-air interface is

$$k_{\mathrm{sp}} = \frac{\omega}{c}\left(\frac{\varepsilon_{\mathrm{M}}}{\varepsilon_{\mathrm{M}}+1}\right)^{1/2}, \tag{1}$$

where $\varepsilon_{\mathrm{M}} = \varepsilon' + \mathrm{i}\varepsilon''$ is the complex dielectric constant of the metal.

The simplest 'photonic surface' is an ordinary diffraction grating having a period Λ close to half of the wavelength λ ($\Lambda \sim \lambda/2$). When the projection of the SP wave vector $\mathbf{k}_{\mathrm{sp}}$ on the normal to the grooves is equal to half the Bragg vector of the grating $\mathbf{g}$, that is if $k_{\mathrm{sp}} \cos(\varphi) = g/2$ (φ is the angle between the vectors $\mathbf{k}_{\mathrm{sp}}$ and $\mathbf{g}$), then Bragg scattering of SPs takes place. The two counter-propagating SP

Journal of Modern Optics ISSN 0950-0340 print/ISSN 1362-3044 online © 2001 Taylor & Francis Ltd
http://www.tandf.co.uk/journals
DOI: 10.1080/09500340110056420

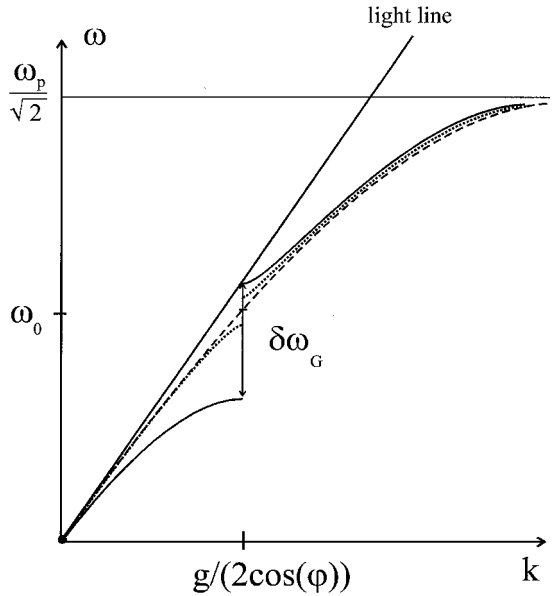

Figure 1. The form of the SP dispersion curve near the gap opened up by the interaction of SP with a periodically corrugated surface. The dashed line shows the SP dispersion curve for a flat metal surface, the dotted line that for a weakly corrugated surface, and the solid line that for a strongly corrugated surface.

modes set up a standing wave and, owing to the different surface charges and field distributions on the grating surface, associated with the two standing-wave solution, a band gap in the dispersion of the mode opens up.

There are several theoretical approaches to describe the SP band gap. A short review of these approaches can be found in [4]. We will use the theory of Mills [5] (see also [6]) as a starting point in our consideration. This theory gives an analytical expression for the SP dispersion relation in the vicinity of the gaps opened by interaction with the periodically corrugated surface. Figure 1 shows the SP dispersion curve for a flat surface (the dashed line) and for corrugated surfaces.

According to Mills, the band gap width $\delta\omega_G$ for gratings with shallow grooves h ($h < \Lambda \equiv 2\pi/g$) is

$$\frac{\delta\omega_G}{\omega_0} = \frac{gh}{(|\varepsilon'|)^{1/2}}\cos(\varphi), \tag{2}$$

and the form of the SP dispersion curve is schematically shown by dotted line in figure 1.

However, the theory of Mills (and other theories) does not describe the situation when the band gap width $\delta\omega_G$ becomes larger than the distance between the SP dispersion curve for a flat surface and the light line (see figure 1, the solid line). The energy distance is given by

$$\frac{\omega - \omega_0}{\omega_0} = \frac{ck - ck[(\varepsilon'+1)/\varepsilon']^{1/2}}{ck[(\varepsilon'+1)/\varepsilon']^{1/2}} \approx -\frac{1}{2\varepsilon'} = \frac{1}{2|\varepsilon'|}. \tag{3}$$

Comparing (2) and (3) one can see that the influence of the light line (that is the influence of the interaction between the SP and light) on the SP dispersion curve becomes important when $h > (g\cos(\varphi)\varepsilon'^{1/2})^{-1}$. If

$$h > \frac{\Lambda}{2\pi\cos(\varphi)(|\varepsilon'|)^{1/2}} \simeq \frac{\lambda}{4\pi\cos^2(\varphi)(|\varepsilon'|)^{1/2}}, \tag{4}$$

then we have to modify the analytic expression for the SP dispersion curve near the band gap. The inequality (4) must be considered only as a first-order estimation, inasmuch as increasing the strength of modulation of a corrugated surface not only results in the band gap becoming wider, but the central frequency is also reduced (see [4] for detail). The inequality (4) is fulfilled even for not very large h. For instance, in the visible region $\varepsilon'_{\mathrm{Ag}} \simeq -18$ ($\lambda = 0.63\,\mu\mathrm{m}$) and, therefore, a modification of the theory is necessary for $h > \lambda/50$ (for $\varphi = 0$).

This modification is especially needed at the middle and the far-infrared regions, where the energy distance between the SP dispersion curve and the light line is vanishingly small. For example, at $\lambda = 10.6\,\mu\mathrm{m}$, $\varepsilon'_{\mathrm{Ag,Au,Cu}} \simeq -4500$ and condition (4), for $\varphi = 0$, becomes $h > \lambda/850$, so the Mills theory is not applicable in this case. A knowledge of the real and imaginary parts of the SP wave vector near the photonic band gap is of more than only theoretical interest. It is of vital importance for estimating the decrease of the SP intensity on the 'photonic surface'. If the photonic surface is used as a mirror for high-power infrared laser radiation, then the decrease in the intensity of SPs can increase the laser damage threshold of such a mirror [7].

The main objective of this paper is to investigate both theoretically and experimentally the behaviour of the real and imaginary parts of the SP wave vector near the band gap under condition (4).

We introduce a physical model of the interaction of light waves with SPs and use the coupled-mode formalism to obtain the SP dispersion relation near the gap in an analytical form, with the emphasis on the physical explanation of the result. The method of interferometric SP spectroscopy is used for the first time to obtain experimentally the real and imaginary part of the SP wave vector near the band gap. We used the wavelength region $\lambda \simeq 10\,\mu\mathrm{m}$ where a discrepancy between the theory of Mills and experiment is present even for a very small h.

The plan of this paper is as follows: section 2 presents the theory. We will start with the theory of Mills and then give our expressions for the SP wave vector near the band gap. Section 3 describes our experimental approach and presents experimental results. In section 4 our experimental data will be discussed and compared with the theoretical results from section 2. We offer some conclusions in section 5.

2. Theory

2.1. *Equation for* k_{sp} *near band gaps from the theory of Mills*

The dispersion relation near the centre of the gap (k_0, ω_0) obtained by Mills [5] in our notation has the representation

$$\left(\delta\omega - \frac{\omega_0\delta k}{k_0 l}\right)\left(\delta\omega + \frac{\omega_0\delta k\cos(2\varphi)}{k_0 l}\right) = \frac{|\varepsilon'|^2\omega_0^2 D}{l^2(\varepsilon'^2 - 1)^2}, \tag{5}$$

where φ is the angle between the SP wave vector and the Bragg vector of the grating,

$$l = l(\omega) = \left\{1 + \frac{\omega}{2|\varepsilon'|(|\varepsilon'| - 1)} \frac{\mathrm{d}\varepsilon'(\omega)}{\mathrm{d}\omega}\right\}_{\omega=\omega_0}, \tag{6}$$

where $\mathrm{d}\varepsilon'(\omega)/\mathrm{d}\omega$ is the derivative of the real part of the dielectric constant with respect to the frequency and

$$D = \frac{k_0^2}{|\varepsilon'|} h^2 |(\varepsilon' - 1)\cos^2(\varphi)|^2. \tag{7}$$

Usually equation (5) is solved for $\delta\omega$ in terms of δk. Our experimental results are represented as $k_{\mathrm{sp}} = k_{\mathrm{sp}}(\varphi)$ at some fixed ω and we have to solve (5) in these terms:

$$\frac{\delta k_\pm}{k_0} = -\frac{\delta\omega l \sin^2(\varphi)}{\omega_0 \cos(2\varphi)} \pm \left(\frac{l^2 \delta\omega^2}{\cos^2(2\varphi)\omega_0^2} - \frac{|\varepsilon'| h^2 k_0^2}{\cos(2\varphi)(\varepsilon' + 1)^2}\right)^{1/2} \cos^2(\varphi). \tag{8}$$

We denote

$$\begin{aligned} \delta\omega &= \omega - \omega_0 = \omega - \frac{gc}{2\cos(\varphi)} \left(\frac{\varepsilon' + 1}{\varepsilon'}\right)^{1/2}, \\ \delta k &= k - k_0 = k - \frac{g}{2\cos(\varphi)}. \end{aligned} \tag{9}$$

The solution of equation (5) in these terms is

$$k_\pm(\varphi, \omega) = \frac{g}{2\cos\varphi} - \frac{l\Delta \sin^2(\varphi)}{2\cos(2\varphi)\cos\varphi} \pm \frac{\varrho^{1/2}}{2\cos(2\varphi)}, \tag{10}$$

where

$$\begin{aligned} \varrho &= -4\left(\frac{\varepsilon'}{\varepsilon' + 1}\right)^2 \kappa^2 \cos(2\varphi) + l^2 \Delta^2 \cos^2(\varphi), \\ \Delta &= \frac{2\omega}{c} \left(\frac{\varepsilon'}{\varepsilon' + 1}\right)^{1/2} \cos(\varphi) - g, \\ \kappa &= \frac{g^2 h}{4(|\varepsilon'|)^{1/2}}. \end{aligned} \tag{11}$$

Equation (10) can be simplified in the limit $l \simeq 1$, $\varepsilon' + 1 \simeq \varepsilon'$ and $\varphi = 0$:

$$k_\pm(0, \omega) \simeq \frac{g}{2} \pm \frac{\mathrm{i}}{2} \left[4\left(\frac{g^2 h}{4(|\varepsilon'|)^{1/2}}\right)^2 - \left(\frac{2\omega}{c} - g\right)^2\right]^{1/2}. \tag{12}$$

Now we will show that a similar dispersion relation can be derived using the coupled-mode formalism for two interacting SP modes. Later, in subsection 2.3, we will extend this formalism to the case of three interacting modes (two of them are SP modes and one is a light mode). This enables us to take into account the interaction between SPs and light waves.

2.2. *Coupled-mode approach: two interacting modes*

At first, following Yariv [8], we will obtain expressions for the behaviour of the wave vector near the band gap in the case of two interacting modes. Let us

consider two electromagnetic modes with complex amplitudes A and B and wave vectors k_a and k_b. These are taken as the eigenmodes of the unperturbed medium so that they represent propagating disturbances

$$\begin{aligned} a &= A \exp [\mathrm{i}(\omega t + k_a z)], \\ b &= B \exp [\mathrm{i}(\omega t - k_b z)], \end{aligned} \tag{13}$$

where A and B are constant. Mode a corresponds to a left $(-z)$ travelling wave while b travels to the right. In the presence of a surface corrugation, power is exchanged between modes a and b. The complex amplitudes A and B in this case are no longer constant but will depend on z. They obey the following relations [8, 9]

$$\begin{cases} \dfrac{\mathrm{d}A}{\mathrm{d}z} = \kappa_{ab} B \exp (-\mathrm{i}\Delta z), \\ \dfrac{\mathrm{d}B}{\mathrm{d}z} = \kappa_{ba} A \exp (+\mathrm{i}\Delta z), \end{cases} \tag{14}$$

where the phase-mismatch constant Δ depends on the wave vectors k_a and k_b as well as on the Bragg vector $\mathbf{g}$ of the coupling grating. The coupling coefficients κ_{ba} and κ_{ab} are determined by the physical situation under consideration.

It is extremely convenient to define A and B in such a way that $|A(z)|^2$ and $|B(z)|^2$ correspond to the power carried by modes a and b, respectively. The conservation of the total power is thus expressed as

$$\frac{\mathrm{d}}{\mathrm{d}z} (|B(z)|^2 - |A(z)|^2) = 0, \tag{15}$$

which, using (14), is satisfied when

$$\kappa_{ab} = \kappa_{ba}^*. \tag{16}$$

On reducing system (14) to one differential equation, we remove the exponential dependence on z and obtain a differential equation of the second order with constant coefficients

$$\frac{\mathrm{d}^2 B(z)}{\mathrm{d}z^2} - \mathrm{i}\Delta \frac{\mathrm{d}B(z)}{\mathrm{d}z} - |\kappa_{ba}|^2 B(z) = 0. \tag{17}$$

Seeking the solution in the form

$$B(z) = \mathrm{const} \exp (\mu z), \tag{18}$$

we obtain the quadratic equation for eigenvalues μ

$$\mu^2 - \mathrm{i}\Delta\mu - |\kappa_{ba}|^2 = 0. \tag{19}$$

The general solution of (14), (17) has the form (excepting the case when $\mu_1 = \mu_2$)

$$B(z) = b_1 \exp (\mu_1 z) + b_2 \exp (\mu_2 z), \tag{20}$$

where

$$\mu_{1,2} = \tfrac{1}{2}\mathrm{i}\Delta \pm \tfrac{1}{2}S, \tag{21}$$

$$S = (4|\kappa_{ba}|^2 - \Delta^2)^{1/2}, \tag{22}$$

and the constants b_1 and b_2 are defined from boundary conditions.

We take mode b to be incident at $z = 0$ on the perturbed region which occupies the space between $z = 0$ and $z = L$. Since mode a is generated by the perturbation we have

$$b(0) = b_0, \quad a(L) = 0. \tag{23}$$

With these boundary conditions we have

$$\begin{aligned} b_1 &= \frac{b_0(S - \mathrm{i}\Delta)}{\exp(SL)(\mathrm{i}\Delta + S) - \mathrm{i}\Delta + S}, \\ b_2 &= \frac{b_0(S + \mathrm{i}\Delta)\exp(SL)}{\exp(SL)(\mathrm{i}\Delta + S) - \mathrm{i}\Delta + S}. \end{aligned} \tag{24}$$

The wave vector k_b' of the perturbed mode receives an addition δk_b to the wave vector k_b of the unperturbed mode b:

$$k_b' = k_b + \delta k_b, \tag{25}$$

where δk_b, in the general case, is given by

$$\delta k_b = -\frac{\mathrm{d}}{\mathrm{d}z}[\text{argument}(b_1 \exp(\mu_1 z) + b_2 \exp(\mu_2 z))]. \tag{26}$$

But inasmuch as $|b_1| \simeq 1$, $|b_2| \simeq 0$ for $\Delta < -2|\kappa_{ba}|$ and $|b_1| \simeq 0$, $|b_2| \simeq 1$ for $\Delta > -2|\kappa_{ba}|$ we can write

$$\begin{aligned} \delta k_b &\simeq \mathrm{i}\mu_1 \quad \text{at} \quad \Delta < -2|\kappa_{ba}|, \\ \delta k_b &\simeq \mathrm{i}\mu_2 \quad \text{at} \quad \Delta > -2|\kappa_{ba}|. \end{aligned} \tag{27}$$

We have obtained the solution in a general form without specifying the nature of the contradirectional coupling between the two modes. Comparing equations (25), (27), (21) and (22) with (12), it is apparent that for SP modes, coupled through the grating, the coupling coefficient κ_{ba} is

$$|\kappa_{ba}| = \frac{g^2 h}{4(|\varepsilon'|)^{1/2}}. \tag{28}$$

From equations (21), (22) and (27) one can see that the maximum negative value of the imaginary part of the SP wave vector is

$$-\mathrm{Im}(k_2) = |\kappa_{ba}|, \tag{29}$$

and it takes place at $\Delta = 0$. The dissipation in mode b is due to an energy transfer to the counter-propagating mode a. From the same equations one can see that the maximum addition to the real part of the SP wave vector occurs at

$$\Delta = \pm 2|\kappa_{ba}|, \tag{30}$$

(at these points $\mathrm{Im}(k_2)$ becomes zero) and is given by

$$\mathrm{Re}(k_{1,2}) = \mp|\kappa_{ba}|. \tag{31}$$

Therefore

$$\frac{\delta k_\mathrm{G}}{k_0} = \frac{\delta k_\mathrm{G}}{(g/2)} = \frac{2|\kappa_{ba}|}{(g/2)} = \frac{gh}{(|\varepsilon'|)^{1/2}}. \tag{32}$$

Here it may be noted that δk_G is the difference between maximum and minimum values of k, which occur at the edges of the *frequency* band gap. Therefore there is no need to use a term 'k-gap' here, because it is really 'ω-gap'

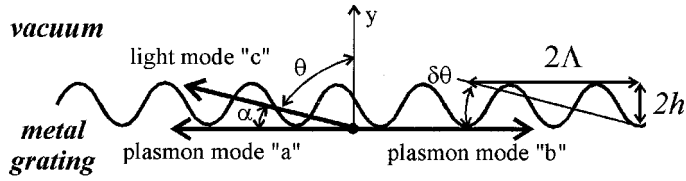

Figure 2. A schematic illustration of the interaction between scattered light wave 'c' and plasmon wave 'b' at the metal grating.

and k becomes the complex value in the gap. We believe that the term 'k-gap' must be reserved for conditions such as 'a medium with modulated gain', where the real 'k-gap' takes place, and frequency ω becomes complex in the 'k-gap' [10].

2.3. *Coupled-mode approach: three interacting modes*

Now we introduce the third interacting mode—light mode c—into system (14). The necessity of the introducing the third mode is explained in figure 2. When $|\mathsf{k}_{sc}| = |\mathsf{k}_{sp} - \mathsf{g}| \leqslant \omega/c$ the energy of SP mode b is leaking out to light mode c, which propagates at a small angle $\alpha = \pi/2 - \theta$ to the surface ($k_{sc} = (\omega/c)\cos(\alpha)$).

Furthermore, for $\alpha < \delta\theta \sim h/\Lambda$ an *inter*action between light mode c and SP mode b takes place. This occurs because, during propagation along the surface at the near-grazing angle, light mode c actually interacts with the modulated medium and can obtain the momentum-g directed along the surface and returns to its original state—to the SP mode b.

So, we have three interacting modes a, b, c:

$$\begin{aligned} a &= A\exp[\mathrm{i}(\omega t + k_a z)], \\ b &= B\exp[\mathrm{i}(\omega t - k_b z)], \\ c &= C\exp[\mathrm{i}(\omega t + k_c z)]. \end{aligned} \tag{33}$$

They obey the following relations

$$\begin{cases} \dfrac{\mathrm{d}A}{\mathrm{d}z} = \kappa_{ab} B\exp(-\mathrm{i}\Delta_{ba} z), \\ \dfrac{\mathrm{d}B}{\mathrm{d}z} = \kappa_{ba} A\exp(\mathrm{i}\Delta_{ba} z) + \kappa_{bc} C\exp(\mathrm{i}\Delta_{bc} z), \\ \dfrac{\mathrm{d}C}{\mathrm{d}z} = \kappa_{cb} B\exp(-\mathrm{i}\Delta_{bc} z), \end{cases} \tag{34}$$

where Δ_{ba} and Δ_{bc} are the phase-mismatch constants between the corresponding modes.

The equation for the conservation of the total power now becomes

$$\frac{\mathrm{d}}{\mathrm{d}z}(|B(z)|^2 - |A(z)|^2 - |C(z)|^2) \simeq 0, \tag{35}$$

which, using (34), is satisfied when

$$\kappa_{ab} \simeq \kappa_{ba}^* \quad \text{and} \quad \kappa_{cb} \simeq \kappa_{bc}^*. \tag{36}$$

Reducing system (34) to one differential equation, we remove the exponential dependence on z and obtain a differential equation of the third order with constant

coefficients. Seeking the solution in the form $B(z) = \text{const}\exp(\mu z)$ we obtain a cubic equation for the eigenvalues μ

$$\mu^3 + \alpha\mu^2 + \beta\mu + \gamma = 0, \tag{37}$$

where the coefficients α, β and γ are

$$\begin{aligned} \alpha &= -\mathrm{i}(\Delta_{ba} + \Delta_{bc}), \\ \beta &= -|\kappa_{ba}|^2 - |\kappa_{bc}|^2 - \Delta_{ba}\Delta_{bc}, \\ \gamma &= \mathrm{i}(|\kappa_{ba}|^2\Delta_{bc} + |\kappa_{bc}|^2\Delta_{ba}). \end{aligned} \tag{38}$$

The general solution of (34) has the form (except the cases when $\mu_i = \mu_j$)

$$B(z) = b_1\exp(\mu_1 z) + b_2\exp(\mu_2 z) + b_3\exp(\mu_3 z), \tag{39}$$

and $\mu_{1,2,3}$ are the solutions of cubic equation (37)

$$\begin{aligned} \mu_1 &= \frac{1}{6}Q^{1/3} - 2\frac{p}{Q^{1/3}} - \frac{\alpha}{3}, \\ \mu_{2,3} &= -\frac{1}{12}Q^{1/3} + \frac{p}{Q^{1/3}} \pm \frac{3^{1/2}}{2}\mathrm{i}\left(\frac{1}{6}Q^{1/3} + 2\frac{p}{Q^{1/3}}\right) - \frac{\alpha}{3}, \end{aligned} \tag{40}$$

where

$$\begin{aligned} Q &= -108q + 12(12p^3 + 81q^2)^{1/2}, \\ p &= \beta - \frac{1}{3}\alpha^2, \\ q &= \gamma - \frac{1}{3}\beta\alpha + \frac{2}{27}\alpha^3. \end{aligned} \tag{41}$$

The constants b_1, b_2 and b_3 are defined from the boundary conditions. If the boundary conditions are such that mode b is incident at $z = 0$ on the perturbed region which occupies the space between $z = 0$ and $z = L$, we have

$$b(0) = b_0, \quad a(L) = 0, \quad c(L) = 0. \tag{42}$$

In this case

$$\begin{aligned} b_1 &= \frac{b_0}{\Sigma}(\mu_2 - \mu_3)(\Delta_{ba} + \mathrm{i}\mu_1)(\Delta_{bc} + \mathrm{i}\mu_1)\exp[(\mu_2 + \mu_3 - \mathrm{i}\Delta_{ba} - \mathrm{i}\Delta_{bc})L], \\ b_2 &= \frac{b_0}{\Sigma}(\mu_3 - \mu_1)(\Delta_{ba} + \mathrm{i}\mu_2)(\Delta_{bc} + \mathrm{i}\mu_2)\exp[(\mu_1 + \mu_3 - \mathrm{i}\Delta_{ba} - \mathrm{i}\Delta_{bc})L], \\ b_3 &= \frac{b_0}{\Sigma}(\mu_1 - \mu_2)(\Delta_{ba} + \mathrm{i}\mu_3)(\Delta_{bc} + \mathrm{i}\mu_3)\exp[(\mu_1 + \mu_2 - \mathrm{i}\Delta_{ba} - \mathrm{i}\Delta_{bc})L], \end{aligned} \tag{43}$$

where

$$\begin{aligned} \Sigma = {} & (\mu_2 - \mu_3)(\Delta_{ba} + \mathrm{i}\mu_1)(\Delta_{bc} + \mathrm{i}\mu_1)\exp[(\mu_2 + \mu_3 - \mathrm{i}\Delta_{ba} - \mathrm{i}\Delta_{bc})L] \\ & + (\mu_3 - \mu_1)(\Delta_{ba} + \mathrm{i}\mu_2)(\Delta_{bc} + \mathrm{i}\mu_2)\exp[(\mu_1 + \mu_3 - \mathrm{i}\Delta_{ba} - \mathrm{i}\Delta_{bc})L] \\ & + (\mu_1 - \mu_2)(\Delta_{ba} + \mathrm{i}\mu_3)(\Delta_{bc} + \mathrm{i}\mu_3)\exp[(\mu_1 + \mu_2 - \mathrm{i}\Delta_{ba} - \mathrm{i}\Delta_{bc})L]. \end{aligned} \tag{44}$$

The wave vector k_b' of the perturbed mode receives an addition δk_b to wave vector k_b of unperturbed mode b—see equation (25)—where δk_b, in the general case, is given by

$$\delta k_b = -\frac{\mathrm{d}}{\mathrm{d}z}[\text{argument}\,(b_1 \exp(\mu_1 z) + b_2 \exp(\mu_2 z) + b_3 \exp(\mu_3 z))]. \tag{45}$$

Equations (39), (40), (38) and (43) give the exact solution of the problem but, instead of these rather unwieldy expressions, it is convenient to have approximate expressions for some important quantities.

In the approximation

$$\Delta_{ba} - \Delta_{bc} = \Delta_{ac} \approx \frac{\omega}{c}\frac{1}{|\varepsilon'|} < |\kappa_{ba}|, |\kappa_{bc}| \tag{46}$$

(this condition is equivalent to (4)) the maximum negative value of the imaginary part of the SP wave vector at $\Delta_{ba} = 0$ is

$$\max[-\mathrm{Im}(k_2), -\mathrm{Im}(k_3)] \simeq (|\kappa_{ba}|^2 + |\kappa_{bc}|^2)^{1/2} - \frac{1}{8}\frac{|\kappa_{bc}|^2(|\kappa_{bc}|^2 + 4|\kappa_{ba}|^2)\Delta_{ac}^2}{(|\kappa_{ba}|^2 + |\kappa_{bc}|^2)^{5/2}}, \tag{47}$$

or if $\Delta_{ac} \sim 0$

$$\max[-\mathrm{Im}(k_2), -\mathrm{Im}(k_3)] \approx (|\kappa_{ba}|^2 + |\kappa_{bc}|^2)^{1/2} \tag{48}$$

(compare this with (29)).

The real part of k_2 in this approximation has the maximum addition at

$$\Delta_{ba} \simeq -2(|\kappa_{ba}|^2 + |\kappa_{bc}|^2)^{1/2} \tag{49}$$

(at this point $\mathrm{Im}(k_2)$ becomes zero)—compare this with (30)—and takes the form

$$\mathrm{Re}(k_2) \simeq +(|\kappa_{ba}|^2 + |\kappa_{bc}|^2)^{1/2}. \tag{50}$$

Inasmuch as at $\Delta_{ba} \simeq +2(|\kappa_{ba}|^2 + |\kappa_{bc}|^2)^{1/2}$ the value $\mathrm{Re}(k_3) \approx -\Delta_{ac}/2$ (~ 0) we have

$$\frac{\delta k_\mathrm{G}}{k_0} = \frac{\delta k_\mathrm{G}}{(g/2)} \approx \frac{(|\kappa_{ba}|^2 + |\kappa_{bc}|^2)^{1/2}}{(g/2)} + \frac{1}{2|\varepsilon'|} \tag{51}$$

(compare this with (32)).

Up to this point we elaborate the coupled-mode approach on the assumption that the SP wave vector k_b is collinear with the grating Bragg vector g ($\varphi = 0$). If $\varphi \neq 0$ then instead of equation (25) one should use

$$|k_b'| \simeq k_b + \delta k_b \cos(\varphi) \tag{52}$$

(it is true at $\delta k_b \ll k_b$), and use the following expressions for Δ_{ba} and Δ_{bc} (see vector diagram on figure 3):

$$\begin{aligned} \Delta_{ba} &= 2k_\mathrm{sp}\cos(\varphi) - g, \\ \Delta_{bc} &= k_\mathrm{sp}\cos(\varphi) + \left\{\left[\frac{\omega}{c}\sin(\theta_\mathrm{max})\right]^2 - [k_\mathrm{sp}\sin(\varphi)]^2\right\}^{1/2} - g \end{aligned} \tag{53}$$

(about θ_max see below, equation (59)).

Let us now determine the other values in the above expressions. The value κ_{ba} has already been determined by equations (28). The coupling coefficient κ_{bc} can be derived from the following consideration: from system (34), ignoring the interaction between modes b and a, one can find that if $\Delta_{bc} \sim 0$ (this takes place at $0 < \alpha < \delta\theta$) the complex amplitude of mode b changes as follows: $B(z) \sim \exp(-|\kappa_{bc}|z)$. Therefore

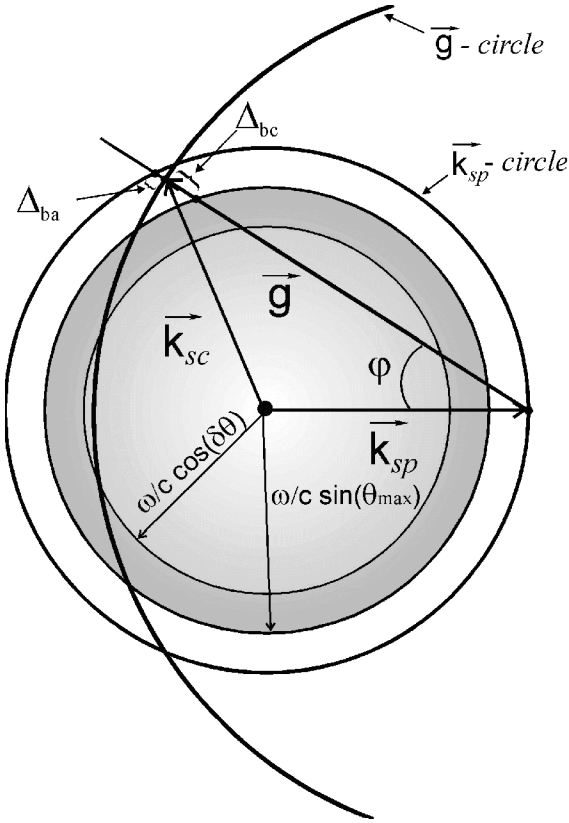

Figure 3. The vector diagram for the scattering of a SP with wave vector $\mathbf{k}_{sp}$ on a grating having Bragg vector $\mathbf{g}$.

$$|\kappa_{bc}| = \gamma_r/2, \tag{54}$$

where γ_r is the constant of the radiative damping of the SP on the grating. For γ_r we used the expression from [11]:

$$\gamma_r \approx \frac{|a_p|^2}{c} = \left| \left(\frac{|Z|\omega\cos(\theta)}{2c} \right)^{1/2} hg \frac{\cos(\varphi)}{\cos(\theta) + Z} \right|^2, \tag{55}$$

where $Z = Z' + iZ'' = 1/\varepsilon_M^{1/2}$ is the surface impedance of the metal. γ_r may be written in the form (55) if angle φ is not very large ($\sin(\varphi) < \cos(\varphi)$). In other words, this means that a transformation of the SP to s-polarized light is neglected. Hereafter we will work with this approximation.

Considering that

$$\begin{aligned} Z' &= \frac{1}{2^{1/2}} \frac{[(\varepsilon'^2 + \varepsilon''^2)^{1/2} + \varepsilon']^{1/2}}{(\varepsilon'^2 + \varepsilon''^2)^{1/2}}, \\ Z'' &= -\frac{1}{2^{1/2}} \frac{[(\varepsilon'^2 + \varepsilon''^2)^{1/2} - \varepsilon']^{1/2}}{(\varepsilon'^2 + \varepsilon''^2)^{1/2}}, \end{aligned} \tag{56}$$

expression (55) can be written in the form

$$\gamma_r = \frac{1}{2c}\frac{(\varepsilon'^2+\varepsilon''^2)^{1/4}\cos^2(\varphi)g^2h^2\cos(\theta)\omega}{(\cos^2(\theta)(\varepsilon'^2+\varepsilon''^2)^{1/2}+2^{1/2}\cos(\theta)((\varepsilon'^2+\varepsilon''^2)^{1/2}+\varepsilon')^{1/2}+1)}. \tag{57}$$

In approximation $\varepsilon'' \ll -\varepsilon'$

$$\gamma_r = -\frac{1}{2}\frac{(-\varepsilon')^{1/2}\cos^2(\varphi)g^2h^2\cos(\theta)\omega}{c(\cos^2(\theta)\varepsilon'-1)}. \tag{58}$$

Function (58) has a sharp maximum at

$$\theta = \theta_{max} = \arccos(|Z|) \simeq \arctan[(-\varepsilon'-1)^{1/2}] \approx \frac{\pi}{2} - \frac{1}{(-\varepsilon')^{1/2}}. \tag{59}$$

In order to appreciate a physical interpretation of this maximum, one must recall Fresnel's formula for p-polarized light. In the Leontovich approximation (see, for example, [12]) it is

$$R_p = \left|\frac{\cos(\theta)-Z}{\cos(\theta)+Z}\right|^2. \tag{60}$$

One can see that at $\theta = \arccos(|Z|)$ equation (60) has a minimum (this is an analogue of the Brewster angle). That is the minimum in the reflection corresponds to the maximum in the plasmon emission.

At this point

$$\gamma_r(\theta_{max}) = \gamma_0 = \frac{\omega}{4c}\cos^2(\varphi)g^2h^2. \tag{61}$$

The substitution $\omega/c \simeq g/(2\cos(\varphi))$ yields

$$\gamma_0 = \tfrac{1}{8}g^3h^2\cos(\varphi). \tag{62}$$

We will proceed as follows: for $\theta > \theta_{max}$, i.e. for

$$\varphi < \varphi_0 = \arccos\left(\frac{k_{sp}^2+g^2-(\omega\sin(\theta_{max})/c)^2}{2k_{sp}g}\right), \tag{63}$$

(see figure 3) we will use equation (58) to determine κ_{bc} and put $\Delta_{bc}=0$; but for $\theta \leqslant \theta_{max}$, i.e. for $\varphi \geqslant \varphi_0$, we will use equation (62) to determine κ_{bc} and will use Δ_{bc} given by equation (53) (such behaviour of the phase-mismatch constant may be described by the following single analytical expression: $1/2\Delta_{bc} - 1/2(\Delta_{bc}^2+d)^{1/2}$, where Δ_{bc} was taken from equation (53) and $d \to 0$).

When condition (4) is satisfied one must use for estimates equations (50), (51) and (47) instead of (31), (32) and (29), respectively. The physical reason for the appearance of the coupling coefficient between SPs and light modes (κ_{bc}) in the new equations is as follows: it is well known that the dominant contribution to the change of the SP wave vector near the gaps comes from a process in which the SP with wave vector $\mathbf{k}_{sp}$ is scattered into an intermediate state with wave vector $\mathbf{k}_{sc} = \mathbf{k}_{sp} - \mathbf{g}$ and then backscattered into the initial state by a second interaction with the periodic surface structure. This process causes a change of the SP phase velocity and thus also of the SP wave vector. When condition (4) is satisfied, not only the SP modes, but also the light modes (which propagate at near-grazing angles $0 < \alpha < \delta\theta \sim h/\Lambda$ to the surface) act as intermediate states for SPs.

One can see that $|\kappa_{bc}| \sim h^2$, while $|\kappa_{ba}| \sim h$ and therefore at $h \to 0$ the coupled-mode solution for three modes transforms to the coupled-mode solution for two modes (i.e. becomes similar to the theory of Mills).

3. Experiment

3.1. *Grating*

The diffraction grating was made on a silicon wafer by the method of photolithography followed by etching, and, was coated by a 380 nm layer of silver. The period of the grating is equal to $\Lambda = (5.3008 \pm 0.0005)\,\mu\text{m}$, the groove depth: $H = 0.24\,\mu\text{m}$, the groove width: $\Lambda - s = 1.41\,\mu\text{m}$, the grating dimension is $10\,\text{mm} \times 10\,\text{mm}$. The profile of our grating was recorded by a commercial scanning probe microscope 'Solver P-47' of the firm 'NT-MDT' [13] (using needles with a radius of curvature $\sim 10\,\text{nm}$) and it is presented in figure 4. The value of the grating period with the accuracy mentioned above was obtained from diffraction measurements using He-Ne laser radiation.

In our theoretical approach we consider the sinusoidal shape of the grating, whereas the present grating is rectangular. We will proceed as follows: we resolve the grating for several Fourier components $y(z) = Hs/\Lambda + \sum_n h_n \cos(ngz)$ with amplitudes given by

$$h_n = \frac{2H}{n\pi} \sin\left(n\pi \frac{s}{\Lambda}\right). \tag{64}$$

The amplitude of the first Fourier component $h = h_1$ ($h_1 \simeq 0.113\,\mu\text{m}$ in our case) is used to find a splitting of the SP dispersion curve in our theory. The presence of

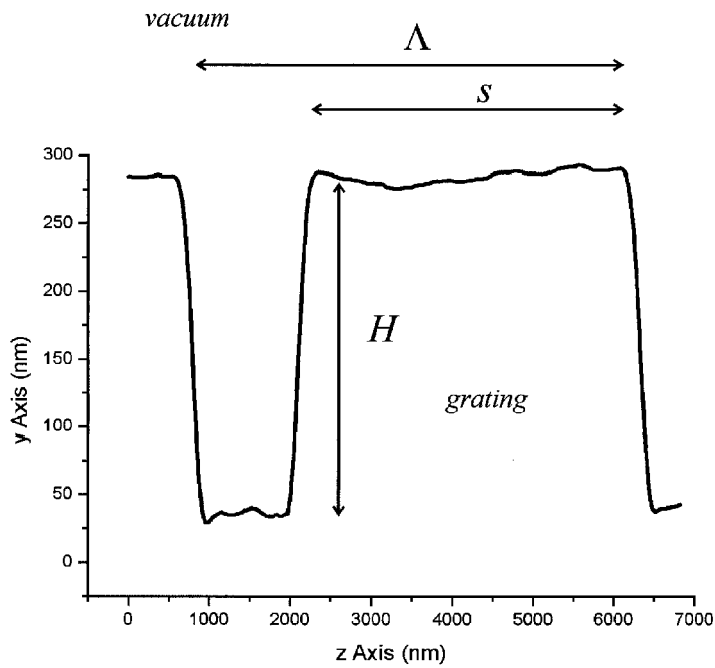

Figure 4. The profile of the grating under study recorded by a scanning probe microscope.

the remaining Fourier components leads to a uniform shift of this curve. The value of this shift can be estimated using a theory developed by Kretschmann and Kröger [14]:

$$\Delta k_{sp} = \sum_n \frac{1}{2} h_n^2 \frac{\omega_0^3}{c^3} \oint g(\mathbf{k} - \mathbf{k}_0) A(\mathbf{k}, \mathbf{k}_0)\, d^2\mathbf{k}, \tag{65}$$

where $g(\mathbf{k} - \mathbf{k}_0) = 0.5(\delta(\mathbf{k} - \mathbf{k}_0 - \mathbf{g}_n) + \delta(\mathbf{k} - \mathbf{k}_0 + \mathbf{g}_n))$ (here δ is the Dirac function) and $A(\mathbf{k}, \mathbf{k}_0)$ is given in [14]. In our numerical calculations the first thirty Fourier components ($n = 30$) were taken into account (it is enough to approximate the real shape of the grating, so one can see from figure 4 that the radius of curvature of the grating edges $\geqslant 20$ nm, while $h_{30} \sim 5$ nm). In this case $\Delta k_{sp} \approx 1.38\,\text{rad cm}^{-1}$.

The direction of SP propagation on the surface of the grating was changed by rotation of the grating. This allowed us to change the angle φ (see figure 3) between the SP wave vector and the Bragg vector of the grating. The grating holder was mounted on a rotating table capable of $1/60^\circ$ resolution inside the unit for SP excitation.

3.2. *Optical system and measurements*

Interferometric phase SP spectroscopy with aperture excitation was used to measure the propagation parameters of SP on the grating surface [15]. The scheme of this experiment is shown in figure 5.

To launch the SP in the 10 μm spectral range on the grating surface CO_2 laser radiation corresponding to spectral lines P(10)-P(28) and R(10)-R(26) is used. The corresponding wavelengths of the radiation are in the spectral ranges 937-953 cm^{-1} and 969-980 cm^{-1}. The CO_2 laser radiation was focused by a cylindrical lens on the aperture gap between the sample surface and the razor blade (see figure 5). A part of the radiation was transformed into SP which propagates along the grating surface; another part travels in the form of a spreading packet of bulk radiation. To convert the SP passing through the grating into bulk radiation the surface behind the grating was partially covered with a thin dielectric overlayer (a 5 μm thick film of polystyrene). At this impedance step the SP was transformed into bulk radiation [16] and interfered with the bulk radiation diffracted at the aperture. The resulting interference pattern contains information about the SP

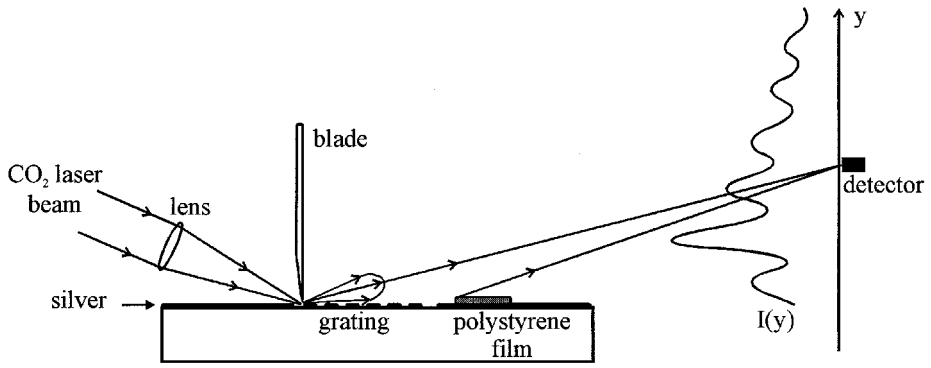

Figure 5. The optical scheme for measurements of SP propagation parameters.

propagation parameters (real and imaginary parts of SP wave vector) on the surface under study. The interference pattern is registered by a detector moving in the direction perpendicular to the sample surface. Joint processing of several interferograms obtained at a fixed frequency for various values of distances covered by the SP allows one to determine the SP wave vector in the given direction of the SP propagation. The SP damping was obtained from the modulation depth of the interference pattern [15].

3.3. *Results*

We have measured the dependence of the propagation parameters of SP on the rotational angle of the grating near the SP band gap. The dispersion curve of SP in the IR region differs from the light line by only 10^{-4}-10^{-3}. Figure 6 displays the experimentally measured difference between the real part of the SP wave vector and the wave vector of bulk radiation with wavelength 974.62 cm^{-1} as a function of the rotational angle of the grating. It is seen that $\mathrm{Re}\,(k_{sp})$ exceeds the wave vector of bulk radiation ω/c and changes from $1.000\,12\omega/c$ to $1.0019\omega/c$. The resonance angle of Bragg scattering at the given frequency for the grating under study is indicated by the arrow in figures 6 and 7. The wave vector of SP propagating on the smooth part of the same silver-covered silicon surface was measured

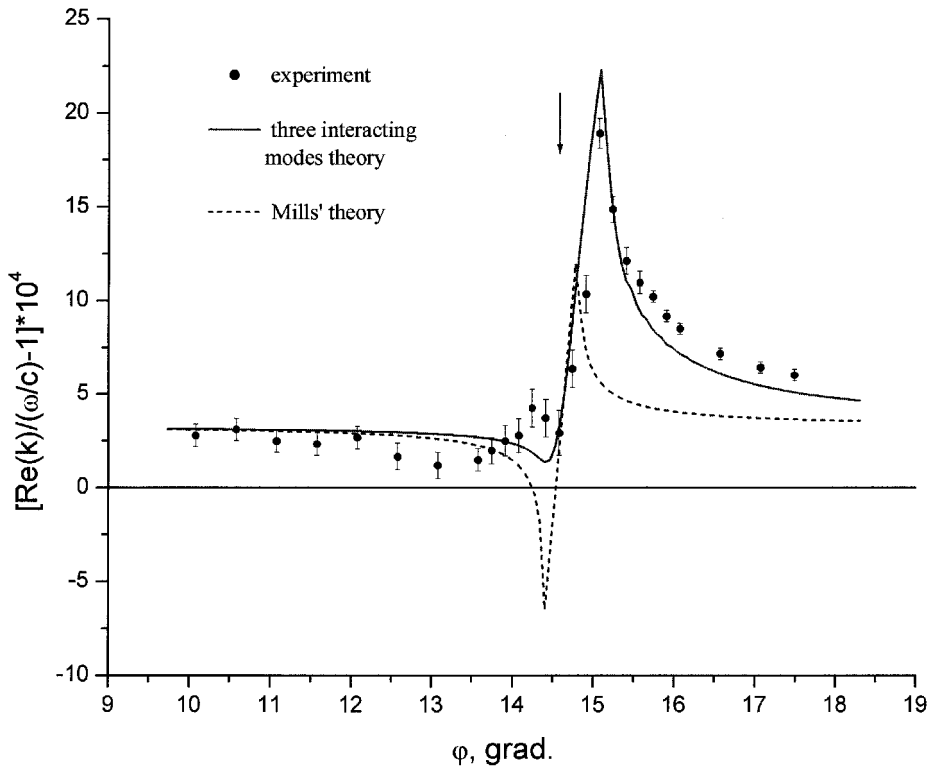

Figure 6. The real part of the SP wave vector on a silver grating as a function of the angle φ between the SP propagation direction and the Bragg vector of the grating. The experimental values are represented by circles (the error bar indicates the accuracy of the measurements). The dashed line corresponds to Mills' theory and the solid line to the coupled-mode approach with three interacting modes.

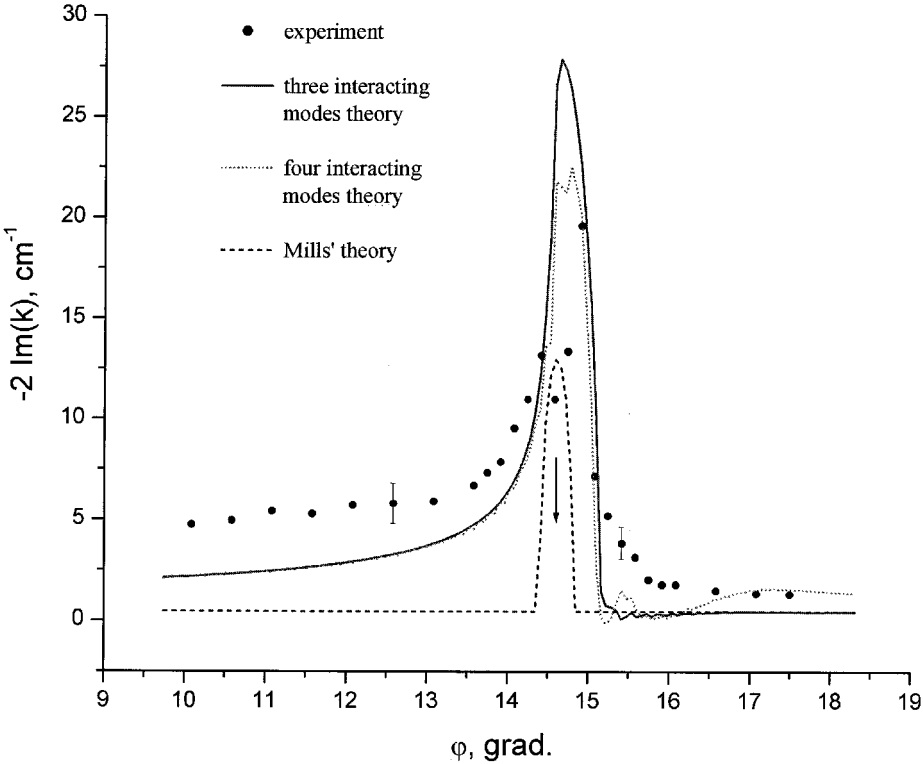

Figure 7. The imaginary part of the SP wave vector on a silver grating as a function of the angle φ between the SP propagation direction and the Bragg vector of the grating. The experimental values are represented by circles, the dashed line corresponds to Mills' theory, the solid line to the coupled-mode approach with three interacting modes and the dotted line to that with four interacting modes.

also by the method of interferometric phase SP spectroscopy: $\mathrm{Re}\,(k_{\mathrm{sp}}) = (1.000\,102 \pm 0.000005)\omega/c$ (at wavelength 974.62 cm^{-1}).

The imaginary part of the SP wave vector determines the SP damping along the surface. The modulation depth of the measured interference pattern depends on the SP damping on the grating and was used to obtain the angular dependence of the imaginary part of the SP wave vector presented in figure 7. So we examined experimentally how the real and imaginary parts of the SP wave vector near the band gap depend on the relative orientation of the Bragg vector of the metal grating and the propagation direction of the SP.

4. Discussion

In figures 6 and 7 our experimental data and theoretical curves calculated from the theory of Mills (equation (10))—the dashed line—and from coupled-mode approach involving three interacting modes (section 2.3)—the solid line—are presented together. From these figures one can see that there is no satisfactory agreement between Mills' theory and the experimental points in the case under consideration, whereas the presented theory gives a much better fit to the experimental data. However, from figure 7 one can see that the coupled-mode theory

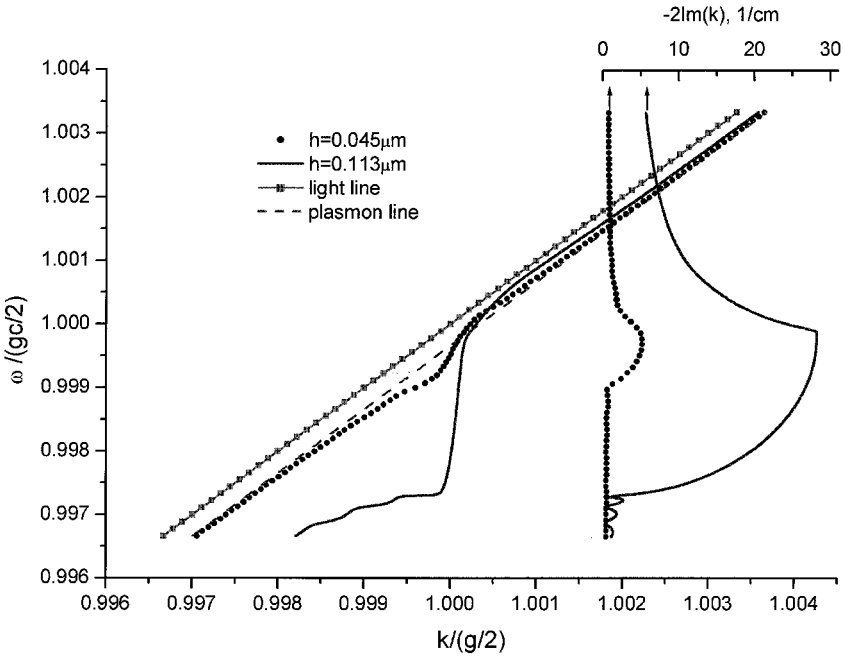

Figure 8. The theoretically calculated dispersion curves of SP on the grating at $\varphi = 0$ with different corrugation amplitudes h of the first Fourier component. The dashed line shows the SP dispersion curve for a flat metal surface, the dotted line that for $h = 0.045\,\mu m$ and the solid line that for $h = 0.113\,\mu m$ (it is the real amplitude of our grating).

with three interacting modes gives a slightly higher value for the imaginary part of the SP wave vector in the centre of the gap. In order to provide a more satisfactory description, a model with four interacting modes—the dotted line—was used (see Appendix for details). From the results presented it can be seen that for gratings usually used in the IR region (where the inequality (4), as a rule, is always fulfilled) Mills' theory is inadequate, while the suggested theory is in good agreement with experiment.

The presented theoretical results can be represented not only in the form $k_{sp} = k_{sp}(\varphi)$ at some fixed ω, but also as $k_{sp} = k_{sp}(\omega)$ at some fixed φ (i.e. as the ordinary SP dispersion curve). To illustrate it in figure 8 we present the theoretically calculated dispersion curves of SP on the grating at $\varphi = 0$ with different corrugation amplitudes h of the first Fourier component. The dashed line shows the SP dispersion curve for a flat metal surface, the dotted line that for $h = 0.045\,\mu m$ and the solid line that for $h = 0.113\,\mu m$ (it is the real amplitude of our grating). From this figure one can see that the shape of the dispersion curve is perceptibly asymmetric (i.e. differs from the Mills theory) even at $h = 0.045\,\mu m$ (i.e at $\lambda/235$).

5. Conclusions

To describe the dispersion relation of SPs near photonic band gaps a physical model based on the coupled-mode approach involving three interacting modes

(two of them are SP modes and one is a light mode) is developed. The inclusion of the interaction between bulk light waves and SPs allows us to describe the experimental data for SP propagation parameters in the IR region. The analytical expression obtained on the basis of this model can be used to determine the form of the SP dispersion curve near the band gap for gratings with the actually used amplitudes of the corrugations. Equations (51) and (48) (using (28), (54) and (62)) can be used for estimations of the dispersion curve splitting and SP damping on gratings in the case under consideration.

Acknowledgments

The authors thank Professor V .A. Yakovlev for useful discussions and Dr A. A. Zhukov for supplying the silicon gratings. The present research was supported by the Russian Foundation for Basic Research and by the program 'Fundamental spectroscopy' of the Russian Ministry of Science.

Appendix: four interacting modes

The fourth mode—the light one d—is symmetrical to the light mode c with respect to the coordinate axis y (see figure 2), i.e. it propagates to the right at a near-grazing angle to the surface. In an 'idealized' case (if an initial source excites only one undamped plasmon wave b on an infinite grating) the intensity of this mode is vanishingly small. But in real experiments the intensity of the light mode d is non-zero, and this mode should be taken into account to describe some fine effects, especially in recording the transmission and reflection of SPs on Bragg gratings [17].

If all interactions between all four modes are taken into account, the corresponding system of differential equations cannot be solved in an analytical form. For this reason we take into account only the main (the strongest) interactions between the four modes. In this case we have four interacting modes a, b, c, d:

$$\begin{aligned} a &= A\exp\left[\mathrm{i}(\omega t + k_a z)\right], \\ b &= B\exp\left[\mathrm{i}(\omega t - k_b z)\right], \\ c &= C\exp\left[\mathrm{i}(\omega t + k_c z)\right], \\ d &= D\exp\left[\mathrm{i}(\omega t - k_d z)\right], \end{aligned} \tag{A 1}$$

which obey relations of the type

$$\begin{cases} \dfrac{\mathrm{d}A}{\mathrm{d}z} = \kappa_{ab} B\exp\left(-\mathrm{i}\Delta_{ba} z\right) + \kappa_{ad} D\exp\left(-\mathrm{i}\Delta_{da} z\right) \\ \dfrac{\mathrm{d}B}{\mathrm{d}z} = \kappa_{ba} A\exp\left(\mathrm{i}\Delta_{ba} z\right) + \kappa_{bc} C\exp\left(\mathrm{i}\Delta_{bc} z\right) \\ \dfrac{\mathrm{d}C}{\mathrm{d}z} = \kappa_{cb} B\exp\left(-\mathrm{i}\Delta_{bc} z\right) \\ \dfrac{\mathrm{d}D}{\mathrm{d}z} = \kappa_{da} A\exp\left(\mathrm{i}\Delta_{da} z\right), \end{cases} \tag{A 2}$$

where Δ_{ba}, Δ_{bc} and Δ_{da} are the phase-mismatch constants between the corresponding modes.

From the equation for the conservation of the total power one can obtain

$$\kappa_{ab} \simeq \kappa_{ba}^{*}\ ; \quad \kappa_{cb} \simeq \kappa_{bc}^{*}\ ; \quad \kappa_{ad} \simeq \kappa_{da}^{*}. \tag{A 3}$$

Reducing system (A 2) to one differential equation, we remove the exponential dependence on z and obtain a differential equation of the fourth order with constant coefficients. Seeking the solution in the form $B(z) = \text{const}\exp(\mu z)$ we obtain an equation for the eigenvalues μ of the fourth order

$$\mu^4 + \alpha\mu^3 + \beta\mu^2 + \gamma\mu + \epsilon = 0, \tag{A 4}$$

where the coefficients are

$$\begin{aligned}
\alpha &= -\mathrm{i}(\Delta_{bc} + 2\Delta_{ba} - \Delta_{da}),\\
\beta &= -|\kappa_{ba}|^2 - |\kappa_{da}|^2 - |\kappa_{bc}|^2 - 2\Delta_{ba}\Delta_{bc} + \Delta_{da}\Delta_{ba} + \Delta_{da}\Delta_{bc} - \Delta_{ba}^2,\\
\gamma &= \mathrm{i}(|\kappa_{ba}|^2(\Delta_{bc} + \Delta_{ba} - \Delta_{da}) + |\kappa_{bc}|^2(2\Delta_{ba} - \Delta_{da})\\
&\quad + |\kappa_{da}|^2\Delta_{bc} + \Delta_{ba}\Delta_{bc}(\Delta_{ba} - \Delta_{da})),\\
\epsilon &= (|\kappa_{bc}|^2\Delta_{ba} + |\kappa_{ba}|^2\Delta_{bc})(\Delta_{ba} - \Delta_{da}) + |\kappa_{da}|^2|\kappa_{bc}|^2.
\end{aligned} \tag{A 5}$$

The general solution of (A 2) has the form (except the cases when $\mu_i = \mu_j$)

$$B(z) = b_1\exp(\mu_1 z) + b_2\exp(\mu_2 z) + b_3\exp(\mu_3 z) + b_4\exp(\mu_4 z), \tag{A 6}$$

where $\mu_{1,2,3,4}$ are solutions of equation (A 4)

$$\mu_{\substack{1\\2\\3\\4}} = \frac{\pm(2\xi)^{3/2} \pm 2\left(-2\xi^3 - 2p\xi \mp 2^{1/2}\xi^{3/2}q\right)^{1/2}}{4\xi} - \frac{1}{4}\alpha, \tag{A 7}$$

with

$$\begin{aligned}
\xi &= S^{1/3} - \frac{R}{3S^{1/3}} - \frac{p}{3},\\
S &= -\frac{1}{2}Q + \frac{1}{18}(12R^3 + 81Q^2)^{1/2},\\
Q &= -\frac{1}{108}p^3 - \frac{1}{8}q^2 + \frac{1}{3}pr,\\
R &= -\frac{1}{12}p^2 - r,\\
p &= \beta - \frac{3}{8}\alpha^2,\\
q &= \gamma - \frac{1}{2}\beta\alpha + \frac{1}{8}\alpha^3,\\
r &= \epsilon - \frac{1}{4}\gamma\alpha + \frac{1}{16}\beta\alpha^2 - \frac{3}{256}\alpha^4.
\end{aligned} \tag{A 8}$$

The constants b_1, b_2, b_3 and b_4 are determined from the boundary conditions. Equations for these constants are cumbersome and are not written here.

The wave vector k_b' of the perturbed mode receives an addition δk_b to the wave vector k_b of the unperturbed mode b, see equation (52), where δk_b, in the general case, is given by

$$\delta k_b = -\frac{\mathrm{d}}{\mathrm{d}z}[\text{argument}\,(b_1 \exp(\mu_1 z) + b_2 \exp(\mu_2 z) + b_3 \exp(\mu_3 z) + b_4 \exp(\mu_4 z))] \tag{A 9}$$

or, which is the same as,

$$\delta k_b = \mathrm{i}\frac{\dfrac{\mathrm{d}}{\mathrm{d}z}(b_1 \exp(\mu_1 z) + b_2 \exp(\mu_2 z) + b_3 \exp(\mu_3 z) + b_4 \exp(\mu_4 z))}{(b_1 \exp(\mu_1 z) + b_2 \exp(\mu_2 z) + b_3 \exp(\mu_3 z) + b_4 \exp(\mu_4 z))}. \tag{A 10}$$

For the new quantities in the presented equations the obvious relations $|\kappa_{da}| \simeq |\kappa_{bc}|$ and $\Delta_{da} = -\Delta_{bc}$ can be used. The solution obtained has been used to derive the imaginary part of the SP wave vector (the dotted line on figure 7).

References

[1] Yablonovitch, E., 1993, *J. opt. Soc. Am.* B, **10,** 283.
[2] Barnes, W. L., Kitson, S. C., Preist, T. W., and Sambles, J. R., 1997, *J. opt. Soc. Am.* A, **14,** 1654.
[3] Raether, H., 1977, *Physics of Thin Films*, Vol. 9 (New York: Academic Press), p. 145.
[4] Barnes, W. L., Preist, T. W., Kitson, S. C., and Sambles, J. R., 1996, *Phys. Rev.* B, **54,** 6227.
[5] Mills, D. L., 1977, *Phys. Rev.* B, **15,** 3097.
[6] Maradudin, A. A., 1982, *Surface Polaritons*, edited by V. M. Agranovich and D. L. Mills (Amsterdam: North-Holland).
[7] Konopsky, V. N., 2000, *Opt. Laser Technol.*, **32,** 15.
[8] Yariv, A., 1973, *IEEE J. quantum Electron.*, **QE9,** 919.
[9] Kogelnik, H., 1975, *Integrated Optics*, edited by T. Tamir (Berlin: Springer-Verlag).
[10] Kogelnik, H., and Shank, C. V., 1972, *J. appl. Phys.*, **43,** 2327.
[11] Gandelman, G. M., and Kondratenko, P. S., 1983, *Sov. Phys. JETP Lett.*, **38,** 291 [1983, *Pis'ma v ZhETF*, **38,** 246 (in Russian)].
[12] Senior, T. B. A., 1960, *Appl. Sci.* Res. Sec. B, **8,** 418.
[13] http://www.ntmdt.ru.
[14] Kretschmann, E., and Kröger, E., 1976, *Phys. status solidi* (b), **76,** 515.
[15] Alieva, E. V., Beitel, G., Kuzik, L. A., Sigarev, A. A., Yakovlev, V. A., Zhizhin, G. N., van der Meer, A. F. G., and van der Wiel, M. J., 1997, *Appl. Spectrosc.*, **51,** 584.
[16] Schlesinger, Z., and Sievers, A. J., 1980, *Appl. Phys. Lett.*, **36,** 409.
[17] Alieva, E. V., and Konopsky, V. N., to be published.